A Single-Material Logical Junction Based on 2D Crystal PdS_2

*Mahdi Ghorbani-Asl, Agnieszka Kuc, Pere Miró, and Thomas Heine**

Since the 1970s, Moore's law[1] marks the progress of miniaturization in the computer industry. Multiple times its end has been prophesized[2,3] as consequence of the presence of quantum effects in the small-scale structures which result in tunnel leakage currents. However, until today, semiconductor industry was able to maintain Moore's law due to ongoing technological progress.

Conventional silicon-based transistors with an extension as small as 3 nm have been reported,[4] and case studies have demonstrated that few-atom[5] and even single-atom[6] transistors are possible. However, high integration of these devices results in strong heat dissipation due to contact resistance and leakage currents. Moreover, for few-atom transistors, electron mobilities are not competitive with those of silicon or alternative semiconductors.

One of the possible ways to continue Moore's law is to use 2D crystals[7] as basis materials, which offer – besides metallic graphene[8] and insulating h-BN – various semiconducting species, e.g. transition metal dichalcogenides (TMDCs).[9] Structural miniaturization to the smallest possible scale, for the direction normal to the crystal plane, is inherent to these materials. A very promising 2D crystal is MoS_2, showing a direct bandgap of 1.8 eV[10] and an electron mobility comparable to that of bulk silicon.[11] Indeed, the first transistor on a 2D crystal has been demonstrated for single-layer MoS_2, and soon after first integrated circuits have been manufactured in the laboratory.[12]

Electrode contacts to the semiconductor may become the next bottleneck for device miniaturization. Whatever electrode material is used, electrical transport across the contact requires electron transmission through the interface between two different crystal lattices, which always causes a contact resistance due to reflections, Schottky barriers, and scattering at the interface. An interesting alternative to traditional metal contacts has been recently proposed by Kappera et al.,[13] who manufactured a transistor on a single-layer MoS_2 nanosheet, where the metallic 1T MoS_2 phase serves as electrode material. However, the MoS_2 1T phase is metastable and at room temperature reconverts to the 2H phase, thus destroying the device. Here, we propose an alternative single-material device, based on PdS_2. A unique feature of 1T PdS_2 (**Figure 1**) is that it was found to be semiconducting as monolayer (ML) with a bandgap of ≈1.1 eV, while it gets semimetallic as bilayer (BL).[14] The material has not yet been realized as mono or bilayer, and it is possible that further competing phases exist.[15] We will show that an ultrathin single-crystal device based on ML and BL PdS_2 shows the desired characteristics of a logical junction, as demonstrated by its calculated *I–V* characteristics. We will show that for channel lengths $l_c \geq 2.45$ nm the leakage current gets negligible and we can ,thus, mark this distance as miniaturization limit for a conventional electron-based logical junction of a typical semiconducting 2D crystal with effective charge carrier masses similar as in prototype TMDC 2H-MoS_2. For smaller channel lengths, the junctions show tunnel diode characteristics.

We have used density-functional theory (DFT) calculations with the Perdew–Burke–Ernzerhof (PBE)[16] exchange-correlation functional, D3 London dispersion interactions,[17] and scalar relativistic treatment as implemented in the ADF/BAND package,[18] applying 2D lattice parameters taken from the fully optimized 1T-PdS_2 bulk (a = 3.068 Å and interlayer distance d = 4.517 Å). Additional electronic structure calculations were performed using G_0W_0[19] and HSE06[20] levels as implemented in the Vienna ab initio simulation package (VASP).[21] Details are given in the Supporting Information.

Coherent transport calculations were performed using the density-functional-based tight-binding (DFTB) method[22] in conjunction with the non-equilibrium Green's function technique, which we have validated and described in detail in previous studies on TMDCs.[23] Electronic parameters are those developed by Wahiduzzaman et al.[24] *I–V* characteristics have been calculated using the Landauer formula.[25] In order to obtain the metallic character of BL in DFTB, the interlayer distance d was slightly compressed by 0.1 Å. The net current through the device within linear response approximation and for a finite bias voltage, V_{Bias}, is expressed as:

$$I(V_{\mathrm{Bias}}) = \frac{2e}{h}\int_{-\infty}^{+\infty} T(\varepsilon, V_{\mathrm{Bias}})\left[f(\varepsilon-\mu_{\mathrm{L}}) - f(\varepsilon-\mu_{\mathrm{R}})\right]\mathrm{d}\varepsilon \quad (1)$$

where f is the Fermi–Dirac distribution function and $\mu_{\mathrm{L,R}} = E_{\mathrm{F}} \pm eV_{\mathrm{Bias}}/2$ represents the chemical potentials of the electrodes. The energy and voltage-resolved transmission function can be calculated using:[25]

$$T(\varepsilon, V_{\mathrm{Bias}}) = Tr\left[\hat{G}_{\mathrm{C}}^{\dagger}\hat{\Gamma}_{\mathrm{R}}\hat{G}_{\mathrm{C}}\hat{\Gamma}_{\mathrm{L}}\right] \quad (2)$$

Dr. M. Ghorbani-Asl, Dr. A. Kuc,
Dr. P. Miró, Prof. T. Heine
Department of Physics and Earth Science
Jacobs University Bremen
Campus Ring 1, 28759 Bremen, Germany
E-mail: thomas.heine@uni-leipzig.de
Dr. M. Ghorbani-Asl
Department of Materials Science and Metallurgy
University of Cambridge
Cambridge CB3 0FS, UK
Dr. A. Kuc, Prof. T. Heine
Wilhelm-Ostwald-Institut für Physikalische
und Theoretische Chemie
University of Leipzig
Linnéstr. 2, 04103 Leipzig, Germany
Dr. P. Miró
Department of Chemical and Biological Engineering
Northwestern University
2145 Sheridan Road, Evanston, IL 60208-3120, USA

DOI: 10.1002/adma.201504274

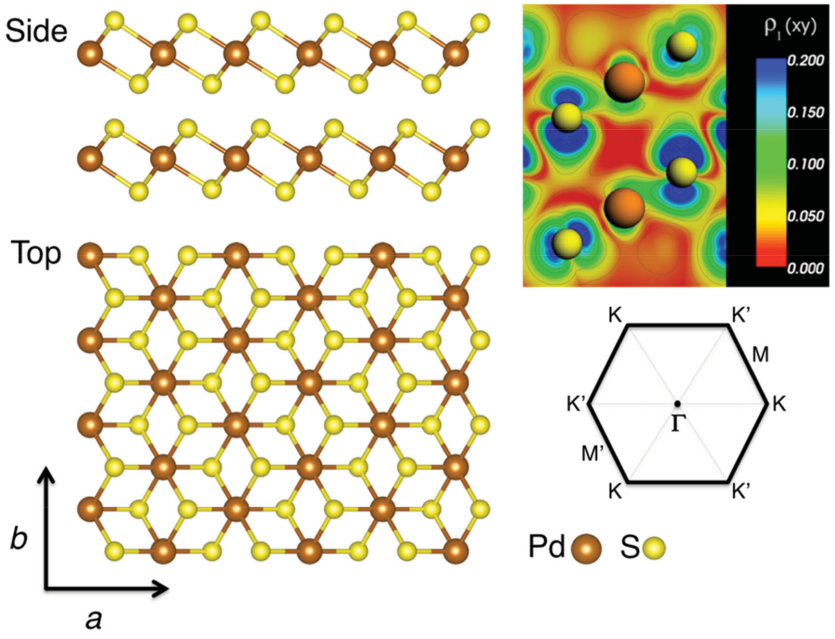

Figure 1. Structure and electronic structure of 1T-PdS_2. (Left) Side and top view of layered 1T-PdS_2. (Right) Calculated contour plots of the charge density (ρ) corresponding to the states with the energy level in the planes perpendicular to the interface in BL-PdS_2 (top). The hexagonal Brillouin zone with the high-symmetry k-points (bottom). Brown: palladium, yellow: sulfur.

where $\hat{G}_C$ is Green's function of the channel region and $\hat{\Gamma}_{L,R}$ are the broadening functions of the left and right electrodes. A finite central region, made of ML-PdS_2, is attached to two semi-infinite electrodes of BL-PdS_2. Both electrodes and the central part are periodic perpendicular to the transport direction. In order to have computationally convenient setup for calculation of broadening functions at the borders, the central region includes small adjacent parts of the leads as buffer layers.[26] The edges of the upper layer at the ML/BL contacts have the structure that is well known for 1T layers. This edge geometry is known to have little influence on the electronic properties of the materials, as recently confirmed by the fast convergence of the electronic properties in Group 4 1T-MX_2 nanoflakes.[27] We have further considered two other stable edge types, both of them performing very similarly to the most stable model (see the Supporting Information), indicating that the geometrical edge structure does not significantly affect the transport results present in this study.

We first reinvestigate the electronic structures of ML and BL PdS_2 by enhancing the level of theory. Our calculations (PBE-BJ-D3, see the Computational Details section in the Supporting Information) on 2D crystal 1T PdS_2 show an indirect bandgap of 0.99 eV from Γ to $(\Gamma - M)/2$ without pronounced SO splitting, thus confirming our earlier results.[14]

The effective electron masses of ML PdS_2 are comparable to those in MoS_2, thus slightly higher than in silicon, while the hole masses are considerably heavier (**Table 1**). These results, together with the expectation of similar scattering mechanisms, suggest similar electron mobilities as in MoS_2.

To understand the strong impact of the interlayer interactions, we projected the charge density contour onto the cross-section plane perpendicular to the BL (Figure 1 right), and observed an accumulation of electron density between the palladium atoms with the sulfur atoms of the neighboring layer. This electron density enhancement between the layers facilitates the transmission of electrons from the BL to the semiconducting ML. The calculated interlayer interaction energy is 0.72 eV per PdS_2 unit, which is about three times stronger than in MoS_2 (≈0.27 eV).

The partial density of states (PDOS) (**Figure 2** and Figure S1, Supporting Information) shows that the metallic character of the BL originates from the S p_z-orbitals (normal to the lattice plane), while the Pd d-orbitals only slightly contribute to the states close to the Fermi level. For DFTB, and also at higher levels of theory, a small bandgap of ≈0.3 eV (HSE06 level) and ≈0.5 eV (G_0W_0) emerges (see Table S1, Supporting Information). To function as electrode in a device, this BL material with such a small bandgap can be made metallic either by doping or by applying pressure, a method that was demonstrated to work for larger-bandgap BL systems MoS_2[29,30] and $MoSe_2$,[31] and which we employ in our DFTB based device simulations.

In our proposed junction concept, the semimetallic BL serves as electrode material contacting the semiconducting ML (Figure S2 in the Supporting Information). Since the whole device is built on the same flake and implemented on a single 2D crystal plane, it has a low contact resistance, making it an attractive candidate for energy-efficient electronic devices. As only one material is used, recycling is greatly facilitated and allows the sustainable use, which is an important aspect when using the precious resource palladium.

The smallest possible lateral extension of a logical diode can be estimated by the smallest channel length l_c, which allows operation without occurrence of leakage currents. **Figure 3** (and Figure S3 in the Supporting Information) shows a schematic representation of the BL/ML/BL PdS_2 junction, the corresponding I–V characteristics, and the electron transmission as function of l_c. In the case of junction with a zigzag edge, some transmission peaks close to the Fermi level occur for the channel length of 1.84 nm, which result in significant leakage currents in the operation mode. For the channel length of 2.45 nm and longer, these peaks completely disappear, and our results predict the I–V characteristics of a diode.

Table 1. Effective masses of electrons and holes of ML-PdS_2, ML-MoS_2, and bulk Si.[28] Values of both spin up and spin down are given. Data obtained from PBE-BJ-D3-SO band structure calculations.

Material	m_e^*/m_0		m_h^*/m_0	
	Down	Up	Down	Up
ML-PdS_2	0.467	0.467	−1.342	−1.342
ML-MoS_2	0.460	0.525	−0.621	−0.542
Si	0.26		−0.36	

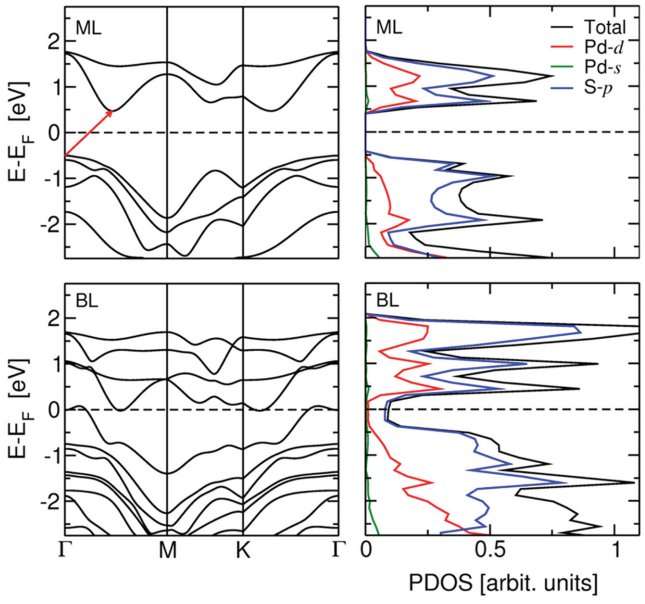

Figure 2. Electronic structure of PdS_2 ML and BL. Band structure and partial densities of states (PDOS) of ML (top) and BL (bottom) PdS_2. PDOS indicates projections on the *d* and *s* orbitals of Pd atoms (red and green) and *p* orbitals of S atoms (blue). The calculations include scalar relativistic effects using spin–orbit interactions.

The edge geometry of the 2nd layer has only minor effects on the *I*–*V* diagram (Figure S3, Supporting Information). Thus, the smallest energy-efficient switching element on the basis of PdS_2 has channel lengths somewhat larger than 2.5 nm, while smaller junctions yield currents below the onset. Those would be prohibitive for energy-efficient switching diodes (or field-effect transistors, FETs), but could be exploited as tunnel diodes.

Figure 3 depicts the *I*–*V* characteristics of our simulated device without gate voltage. While the short channel already shows the typical diode *I*–*V* dependence, small currents are observed at low bias $V_{Bias} < 0.5$ V (see inset). The current gradually enhances with the applied voltage due to the increase of carrier density. The model with $l_c = 2.45$ nm has zero current up to the threshold voltage of ≈0.7 V, presenting the semiconducting diode character. This implies that the electrical transport through longer channels is less detrimental by the contact interaction. Interestingly, the junction shows a negative differential resistance (NDR) feature at different bias voltages, e.g., 0.7–0.8 V, which we attribute to the suppression of the transmission coefficient within the voltage window in that region. The NDR effect can be important for applications including high-frequency oscillators, frequency multipliers, and electrical switches. Our results demonstrate that the peak-to-valley ratio can be modulated with the channel length and the gate voltage.

Figure 3 (and Figure S3 in Supporting Information) also show the effect of a gate voltage on the *I*–*V* characteristics of an exemplary diode with $l_c = 3.07$ nm. The electrostatic potential caused by the gate voltage shifts the energy levels of the channel region, thus changing the current through the system. By increasing the gate voltage, the threshold voltage reduces and for $V_G = 1.0$ V, the switch is closed, showing Ohmic character. The interplay between the energy levels for typical Ohmic and Schottky junctions and the corresponding

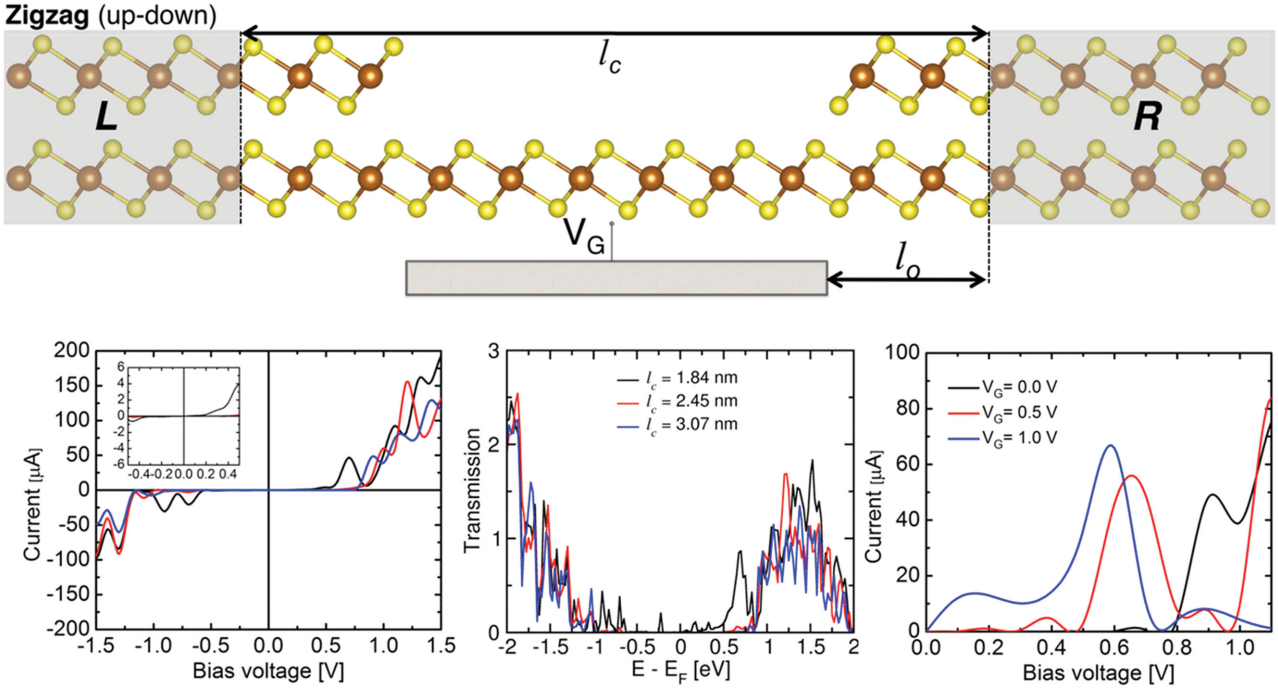

Figure 3. Transport properties of the BL/ML/BL PdS_2 junction. (Top) Schematic representation of a PdS_2-based diode. The BL/ML/BL PdS_2 junction corresponds to the left electrode (*L*)/channel region (*C*)/right electrode (*R*). l_c and l_o correspond to the channel and overlap lengths. Orange: palladium, yellow: sulfur. (Bottom) *I*–*V* characteristics (left) and the transmission coefficients (middle) for BL/ML/BL PdS_2 junction with zigzag up-down edge (cf. Figure S1 in the Supporting Information). (Right) the corresponding *I*–*V* characteristics under different gate voltages for the channel length of $l_c = 3.07$ nm.

I–V characteristics are schematically shown in Figure S4 (Supporting Information).

In conclusion, we propose PdS_2 as interesting material for 2D electronics, as it shows semiconducting properties as a monolayer, but is semimetallic as a bilayer. The interlayer interaction is stronger than in van der Waals crystals and results in more pronounced quantum-confinement effects, which cause this electronic phase transition between ML and BL. The metal–semiconductor dichotomy allows the construction of single-material nanoelectronic devices with low contact resistance and low leakage currents. As the device needs only one material, its recycling is simple, which is economically important as Pd is among the noble metals. The proposed PdS_2 device can have channel lengths of about 2.5 nm and shows the typical *I–V* characteristics of a semiconducting diode that can be controlled by applying a gate voltage. Thus, PdS_2 devices offer all features that are needed for implementing FETs and tunnel diodes in 2D electronic devices. We expect that among the multitude of 2D materials other combinations may qualify for similar, or other unprecedented, properties that offer new device concepts in 2D electronics.

Supporting Information

Supporting Information is available from the Wiley Online Library or from the author. A detailed description of the methodology used in the present work; bandgap values of mono- and bilayer PdS_2 calculated at different levels of theory; projected density of states; transport models and set ups; transmission coefficients and the *I–V* characteristics are shown.

Acknowledgements

The authors are grateful to the grants provided by the Deutsche Forschungsgemeinschaft (HE 3543/18-1) and the European Commission (FP7-PEOPLE-2012-ITN MoWSeS, GA 317451).

Received: September 1, 2015
Revised: October 18, 2015
Published online: December 3, 2015

[1] G. E. Moore, *Electronics* **1965**, *38*, 114.
[2] A. B. Kahng, *IEEE Des. TEST Comput.* **2010**, *27*, 86.
[3] D. Foty, in *2013 Int. Symp. Signals, Circuits and Systems (ISSCS)*, IEEE, Piscataway, NJ, USA **2013**; DOI: 10.1109/ISSCS.2013.6651261.
[4] H. Lee, L. Yu, S.-W. Ryu, J.-W. Han, K. Jeon, D.-Y. Jang, K.-H. Kim, J. Lee, J.-H. Kim, S. C. Jeon, G. S. Lee, J.-S. Oh, Y. C. Park, W. H. Bae, H. M. Lee, J. M. Yang, J. J. Yoo, S. I. Kim, Y.-K. Choi, in *VLSI Technol. 2006. Dig. Tech. Pap. 2006 Symp.*, IEEE, Piscataway, NJ, USA **2006**, pp. 58–59; DOI: 10.1109/VLSIT.2006.1705215.
[5] M. Fuechsle, S. Mahapatra, Z. A. M. Friesen, E. A. Zwanenburg, M. Y. Simmons, *Nat. Nanotechnol.* **2010**, *5*, 502.
[6] M. Fuechsle, J. A. Miwa, S. Mahapatra, H. Ryu, S. Lee, O. Warschkow, L. C. L. Hollenberg, G. Klimeck, M. Y. Simmons, *Nat. Nanotechnol.* **2012**, *7*, 242.
[7] K. S. Novoselov, D. Jiang, F. Schedin, T. J. Booth, V. V Khotkevich, S. V. Morozov, A. K. Geim, *Proc. Nat. Acad. Sci. USA* **2005**, *102*, 10451.
[8] A. H. Castro Neto, F. Guinea, N. M. R. Peres, K. S. Novoselov, A. K. Geim, *Rev. Mod. Phys.* **2009**, *81*, 109.
[9] P. Miro, M. Audiffred, T. Heine, *Chem. Soc. Rev.* **2014**, *43*, 6537.
[10] K. F. Mak, C. Lee, J. Hone, J. Shan, T. F. Heinz, *Phys. Rev. Lett.* **2010**, *105*, 136805.
[11] B. Radisavljevic, A. Kis, *Nat. Mater.* **2013**, *12*, 815.
[12] D. Lembke, S. Bertolazzi, A. Kis, *Acc. Chem. Res.* **2015**, *48*, 100.
[13] R. Kappera, D. Voiry, S. E. Yalcin, B. Branch, G. Gupta, A. D. Mohite, M. Chhowalla, *Nat. Mater.* **2014**, *13*, 1128.
[14] P. Miró, M. Ghorbani-Asl, T. Heine, *Angew. Chem. Int. Ed.* **2014**, *53*, 3015.
[15] Y. Wang, Y. Li, Z. Chen, *J. Mater. Chem. C* **2015**, *3*, 9603.
[16] J. P. Perdew, K. Burke, M. Ernzerhof, *Phys. Rev. Lett.* **1996**, *77*, 3865.
[17] S. Grimme, *J. Comp. Chem.* **2006**, *27*, 1787.
[18] ADF2012, SCM, Theoretical Chemistry, Vrije Universiteit, Amsterdam, The Netherlands, http://www.scm.com (accessed: October 2015).
[19] L. Hedin, *Phys. Rev.* **1965**, *139*, A796.
[20] J. Heyd, G. E. Scuseria, M. Ernzerhof, *J. Chem. Phys.* **2003**, *118*, 8207.
[21] G. Kresse, J. Furthmuller, *Phys. Rev. B* **1996**, *54*, 11169.
[22] G. Seifert, D. Porezag, T. Frauenheim, *Int. J. Quantum Chem.* **1996**, *58*, 185.
[23] T. Heine, *Acc. Chem. Res.* **2015**, *48*, 65.
[24] M. Wahiduzzaman, A. F. Oliveira, P. Philipsen, L. Zhechkov, E. van Lenthe, H. A. Witek, T. Heine, *J. Chem. Theory Comput.* **2013**, *9*, 4006.
[25] S. Datta, *Quantum Transport: Atom to Transistor*, Cambridge University Press, New York **2005**.
[26] A. Ferretti, A. Calzolari, R. Di Felice, F. Manghi, *Phys. Rev. B* **2005**, *72*, 125114.
[27] P. Miro, J. H. Han, J. Cheon, T. Heine, *Angew. Chem. Int. Ed.* **2014**, *53*, 12624.
[28] B. Van Zeghbroeck, Principles of Semiconductor Devices, http://ecee.colorado.edu/~bart/book/effmass.htm (accessed: August 2014).
[29] A. P. Nayak, S. Bhattacharyya, J. Zhu, J. Liu, X. Wu, T. Pandey, C. Jin, A. K. Singh, D. Akinwande, J.-F. Lin, *Nat. Commun.* **2014**, *5*, 3731.
[30] Z.-H. Chi, X.-M. Zhao, H. Zhang, A. F. Goncharov, S. S. Lobanov, T. Kagayama, M. Sakata, X.-J. Chen, *Phys. Rev. Lett.* **2014**, *113*, 36802.
[31] Z. Zhao, H. Zhang, H. Yuan, S. Wang, Y. Lin, Q. Zeng, G. Xu, Z. Liu, G. K. Solanki, K. D. Patel, Y. Cui, H. Y. Hwang, W. L. Mao, *Nat. Commun.* **2015**, *6*, 7312.